A Study of Frequency Selective Fading for a Microwave Line-of-Sight Narrowband Radio Channel

By G. M. BABLER

The spectral and temporal characteristics of a narrowband radio channel subject to multipath fading were estimated from a detailed sampling of channel loss variations. The data base for this characterization was obtained during a 59-day experiment in which the amplitudes of a set of coherent tones spanning a band of 33.55 MHz and centered at 6034.2 MHz were continuously monitored. The more significant observations were:

(i) For fade depths less than 30 dB the frequency selectivity is accurately described by linear and quadratic components (in frequency) of amplitude distortion. The derived statistical distributions of such distortion parameters exhibit slopes of a decade of decrease in probability of occurrence for each 10 dB increase in distortion, for bandwidths greater than 5 MHz.

(ii) For fade depths greater than 30 dB and bandwidths in excess of 5 MHz the amplitude distortion exceeds second order.

(iii) Maximum observed rates of change for the linear and quadratic distortion were 90 and 60 dB/second, respectively.

I. INTRODUCTION

Unusual atmospheric conditions may support microwave propagation over two or more distinct paths between two line-of-sight radio antennas. The various signal paths will typically differ in their propagation delay, thereby permitting constructive and destructive interference at the receiving antenna. When the relative delay is significant with respect to the radio frequency signal period, the interference can be quite selective, with deep nulls in parts of the radio band, and smaller variations at adjacent frequencies. The variation in received power is called fading, and the variation in the amount of fading with radio frequency is known as frequency selective fading.

Experimental data on selective fading are difficult to obtain because of the long time periods (millions of seconds) of continuous measurement required to obtain a sufficient sampling of the fading events for a meaningful characterization. As a result, the experimental literature on the subject generally has been sparse, has been incomplete, or has tended to de-emphasize the magnitude of the propagational effects. W. T. Barnett[1] has explored these frequency effects for discrete microwave signals separated by 20 to 500 MHz, and in an important early study R. L. Kaylor[2] observed maximum amplitude deviations as large as several tens of decibels for the same bandwidths. Because of the ever-increasing emphasis on performance and the need for more efficient use of the microwave frequency spectrum, as well as for other reasons, an extensive experimental program was undertaken in 1970 to more precisely characterize the spectral and temporal effects of frequency selective fading within a narrowband microwave radio channel during a fading season. An additional objective was to obtain information which permits a better understanding of the complex physical processes of multipath fading.

The experiment described in this paper was of 59 days' duration and included the amplitude measurement of 62 uniformly spaced, coherent tones spanning 33.55 MHz at 6 GHz transmitted over a 26.4-mile radio path to Palmetto, Georgia. The tones were sampled five times per second and the results recorded whenever significant activity occurred.

In the following, we present the results of the data analysis and their interpretation. The organization of the report is (*i*) an experimental description, (*ii*) an overview of the fading activity observed, (*iii*) the fading behavior of single tones, (*iv*) a selectivity characterization of multiple tone activity by means of a three-tone amplitude difference technique, (*v*) an error analysis for estimating the higher-order selectivity structure, and (*vi*) observations describing an atypical fading period and comments on the temporal and spatial properties of selective fading.

II. SUMMARY

A listing of the findings follows:

(*i*) The fade depth distributions for individual tones during periods of typical multipath fading were essentially the same and had the expected power law of deep fades with a slope of a decade of probability per 10 dB change in fade depth.[3]

(*ii*) The degree of frequency selectivity was characterized by statistical distributions of linear and quadratic amplitude distortion constructed from the measured amplitudes (in dB) of three uniformly spaced tones spanning different bandwidths in the narrowband channel. The distributions exhibited slopes of a decade of probability per 10 dB change in observed distortion for bandwidths greater than 5 MHz and greater slopes for bandwidths less than 5 MHz. For a bandwidth of 20.35 MHz the linear and quadratic distortions exceeded 15 and 9 dB, respectively, for 10^{-5} of the observation time. As anticipated, the selectivity structure increased with fade depth.

(*iii*) An analysis was made to determine at what fade levels and bandwidths the linear and quadratic amplitude distortion characterization becomes inadequate. The measure of failing was the residual or difference between the observed amplitude-frequency characteristic and a three-term, power series analytic approximation constructed from the linear and quadratic distortions. This study indicated that, for fade depths greater than 30 dB, the amplitude distortion generally exceeded second order.

(*iv*) During deep selective fades the distortion evolves rapidly. The maximum rates of change observed for the linear and quadratic distortion for a bandwidth of 20.35 MHz were 90 and 60 dB/second, respectively.

(*v*) The statistical distributions of amplitude distortion derived from the loss in the narrowband channels as received on two vertically spaced antennas of different beamwidths were found to be nearly identical.

III. EXPERIMENTAL DESCRIPTION

3.1 *The Experiment*

A signal generator located at a microwave station in Atlanta (Fig. 1) generated a field of 62 coherent tones spaced 550 kHz apart and centered on 70.4 MHz. The envelope of the tone field was constant in time and flat to within ±0.5 dB. The transmitter translated the 33.55-MHz-wide tone field to a 6.0342-GHz center frequency, and radiated the signal via a standard horn reflector antenna located 260 feet above the ground. After propagating 26.4 miles along a line-of-sight microwave path (Fig. 2), the test signal was received both by a horn reflector antenna (1.25 degrees half-power beamwidth) 330 feet above ground and a 6-foot dish (2 degrees) located 19 feet 3 inches below the horn, on a microwave relay tower located outside of Palmetto, Georgia.
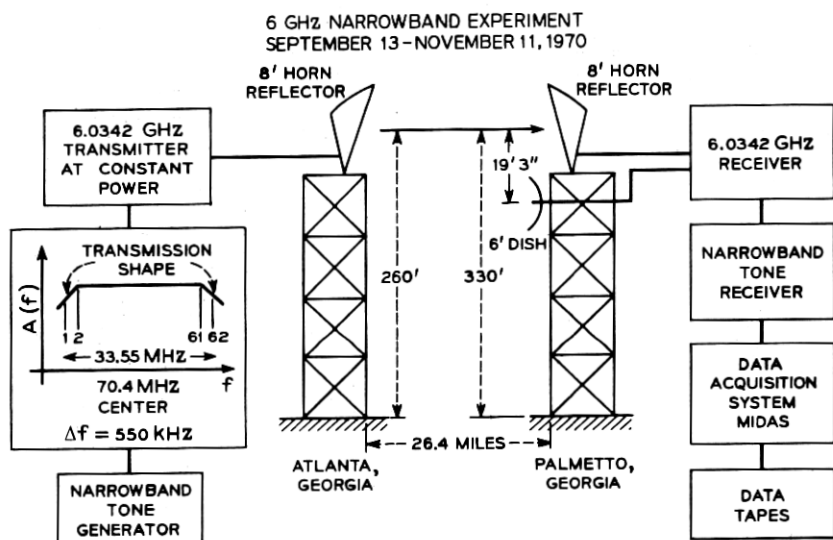
Fig. 1—Experimental layout, Atlanta to Palmetto, Georgia.

Both narrowband tone fields were translated back to 70.4 MHz and a specially designed tone receiver controlled by a multiple input data acquisition system (MIDAS) selected individual tones in a predetermined time sequence for measurement. The subset of tones measured is shown in Fig. 3; each tone was measured every 0.2 second. Using a common detector, the tone amplitudes were converted to dc voltages, quantized into 1-dB steps over a 55-dB range, and recorded on magnetic tape by MIDAS synchronously with timing and tone identification information. The recording rates were 1 sample per 30 seconds, 1 sample per 2 seconds, and 5 samples per second (normal, intermediate, and fast rates) depending on the current fading activity. The higher recording rates were initiated by monitoring the rates of change of tone amplitudes, a necessary step for maintaining a manageable data base for extended surveillance propagation studies.

3.2 Calibration of Reference Levels and Determination of Transmission Shape

The first step in analyzing fading data is to determine the nonfaded reference levels for proper calibration of the received tone amplitudes during fading conditions.

During normal transmission, when the lower atmosphere was well-behaved, the received tone field was nearly identical in shape to the
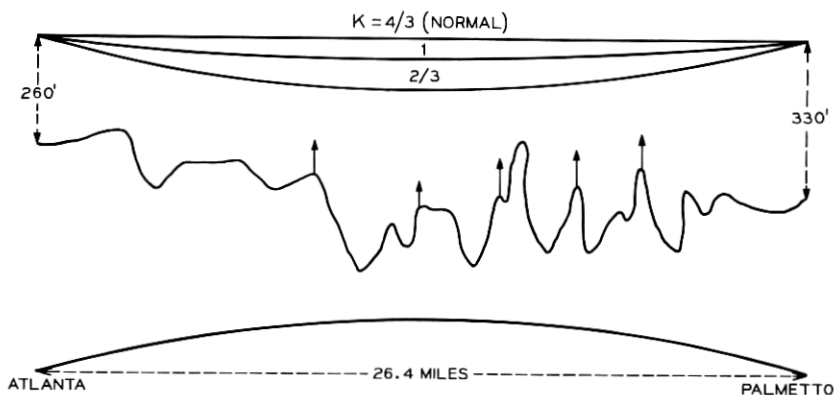
Fig. 2—Atlanta-Palmetto path profile and line-of-sight radio path for the normal (an equivalent earth radius factor $k = 4/3$) and the less frequent ($k = 1, 2/3$) atmospheric configurations. Clearance is adequate even for the extreme case of $k = 2/3$.

transmitted field and was attenuated by the free-space path loss due to the usual spherical radiation spreading. A precise determination of the free-space path loss as well as losses due to radio equipment was done in the usual manner[1] by using midday periods from 12 A.M. to 2 P.M., during which time there was generally no fading. Such quiet periods, selected by visual examination of time plots of received signal levels, were processed by computer to establish the average nonfaded received amplitude levels. These reference levels showed no long-term variations in excess of ± 1 dB throughout the measurement period. By using these results, calibration curves were constructed for the tone receiver detector.
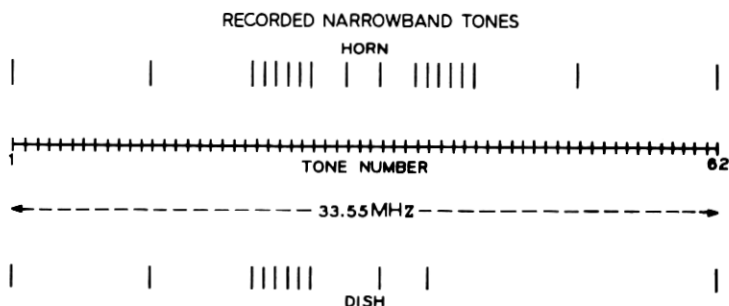

Fig. 3—Subset of 62 tones received on horn reflector and dish antenna measured and recorded serially.

Even during these favorable midday propagation periods, however, the received amplitudes of the tones were undergoing small time-varying random deviations called scintillation. By using specially implemented amplitude measuring capabilities of the tone receiver, amplitude data of all 62 tones were obtained for several 1-hour intervals at a constant rate of 5 measurements per second with an amplitude resolution of 1/8 dB. One such period showing the amplitude statistics of the 2 tones at the extremities of the narrowband is given in Fig. 4. The abscissa is the tone level in dB and the ordinate is the fraction of time that the received tone amplitude has exceeded the indicated level. The horizontal scale is logarithmic and the vertical scale is normal; thus, the scintillation amplitude statistics for both tones are log-normally distributed (normally distributed in dB). The standard deviation of 0.5 dB was found to be independent of tone frequency over the narrowband. The amplitude distribution of the microwave scintillation was found to agree with other experimental studies over the same radio path in previous years.[4]

In addition to the long-term variations in the reference values as well as the short-term scintillation, a third effect was the amplitude deviation across the narrowband arising from the experimental equipment. Figure 5 shows the average received tone level for all 62 tones during the same midday period shown in Fig. 4. As indicated, some tones (e.g., 16, 32) showed spurious amplitude effects. These effects were due to the modulation technique used in the tone generator and such tones were not used in the characterization of the selective fading. In addition, the amplitude depression of the extremities of the tone
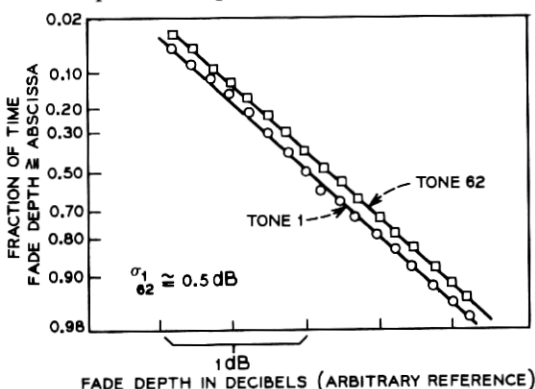

Fig. 4—Amplitude statistics of microwave scintillation for tones 1 and 62 received on horn reflector antenna during a 50-minute midday period on September 21, 1970.
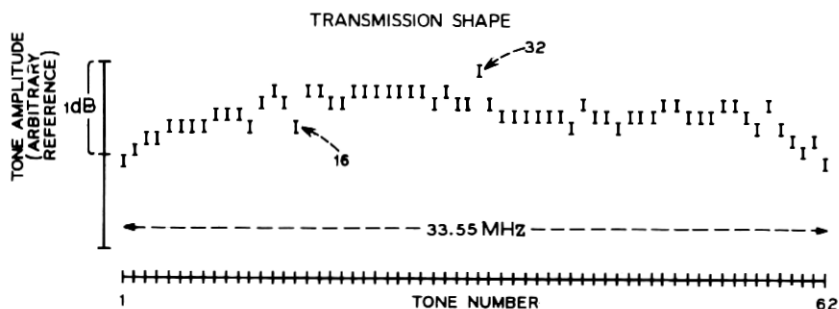
Fig. 5—Transmission shape of narrowband tone field received on horn reflector antenna.

field due to passive filtering were compensated for by suitable modification of the calibration curves for the outer tones.

The reference levels were calibrated in dB relative to midday normal by combining the calibration curves for the detector, the results of the statistical determination of the scintillation effects, and the transmission shape. The rms variation in the reference values for the tones used was estimated to be less than one dB.

IV. OBSERVED FADING ACTIVITY

The fading activity of the narrowband tone fields received by the horn reflector and dish antennas was continuously monitored from September 13 to November 11, 1970, and recorded for almost all of the 59 days (5.1×10^6 seconds). More than 1.8 billion measurements were made and the recorded data base was stored on 20 magnetic tapes. To condense this mass of raw data, a manual preselect was employed which included all periods with any fading in excess of 10 dB. The hour immediately preceding or succeeding each such event was also included. This process condensed the data base to 2 magnetic tapes containing data spanning 1.08×10^6 seconds (21.2 percent) of the total measurement period. This process resulted in a data base with 5 times the fading activity per unit time as compared to that originally measured, and contained all fades in excess of 10 dB. The effects and importance of this apparent increase in normalization of the fading activity will be discussed further in Section V.

An overview of the daily fading activity received on the horn antenna is shown in Fig. 6. The lower half of the figure shows the daily distribution of the fraction of the total time the received amplitude was faded 20 dB for tones 1, 25, 62. The upper half of the figure is for the
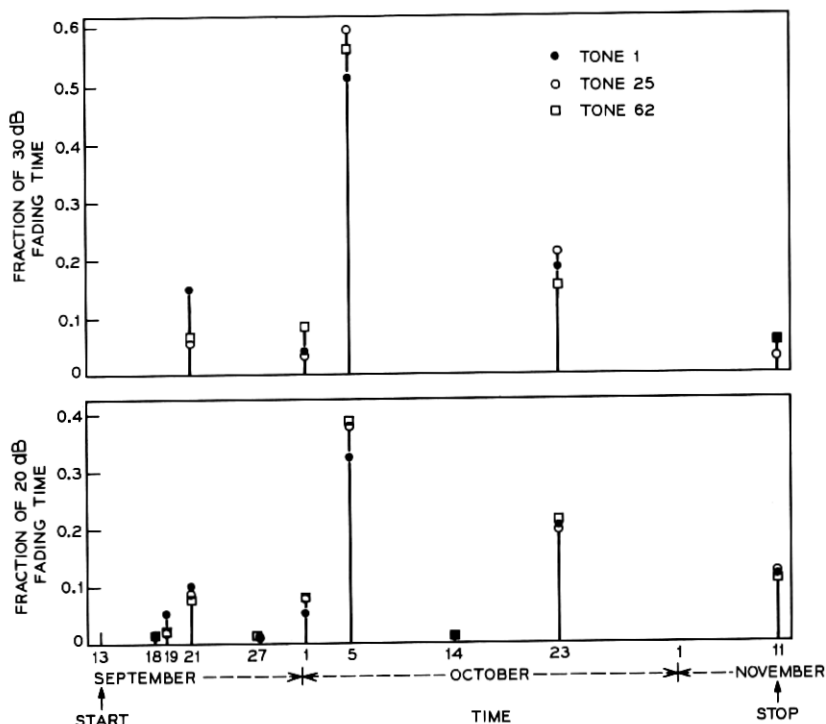
Fig. 6—Daily history of 20 and 30 dB fading activity for tones 1, 25, and 62 during the entire measurement period.

30-dB level. Tone 25 was used instead of tone 32 because of the spurious modulation effects in tone generation mentioned earlier. Several observations can be made from Fig. 6. First, as is typical of line-of-sight multipath fading, the deep fading at these levels occurred in unpredictable bursts; second, higher fading activity occurred in more concentrated bursts and for deeper fades (a rare event phenomena); and third, there was increasingly different fading activity of the closely spaced tones for deeper fades. This last observation is an indication that frequency selective fading is more pronounced for deeper fades as previously observed by Kaylor.[2]

V. FADING BEHAVIOR OF SINGLE TONES

The data were processed by computer to determine the total amount of time during which any tone was faded below a certain level. The resulting fade depth distributions for tones 1, 25, and 62 received on

the horn reflector antenna are given in Fig. 7. The abscissa is the fade depth in dB relative to midday normal and the ordinate is the fraction of the 1.08×10^6 seconds that the tones were faded the indicated amount. It is apparent that these amplitude statistics are not the same below 30 dB with tone 25 in the middle of the narrowband channel having suffered more fading. A preferential amount of fading in the channel, not expected from physical considerations of the overland microwave link, indicates the dominance of one particular fading event and the lack of events at other points in the channel and will now be examined closely.

In a recent study, S. H. Lin[3] has presented a general analysis of the statistical behavior of the envelope of a fading signal. His model indicates that for typical overland line-of-sight microwave links, designed to avoid a single dominant interfering multipath echo, the amplitude V of the received fading signal fades below a specified signal level L according to the following fade depth distribution

$$P(V \leq L)\alpha L^2 \qquad\qquad L \leq 0.1 \text{ (20 dB)} \qquad (1)$$

where fade depth $= -20 \log L$. For the special atypical case of a dominant (single) echo the model indicates the distribution

$$P(V \leq L)\alpha L \qquad\qquad L \leq 0.1 \text{ (20 dB)}. \qquad (2)$$
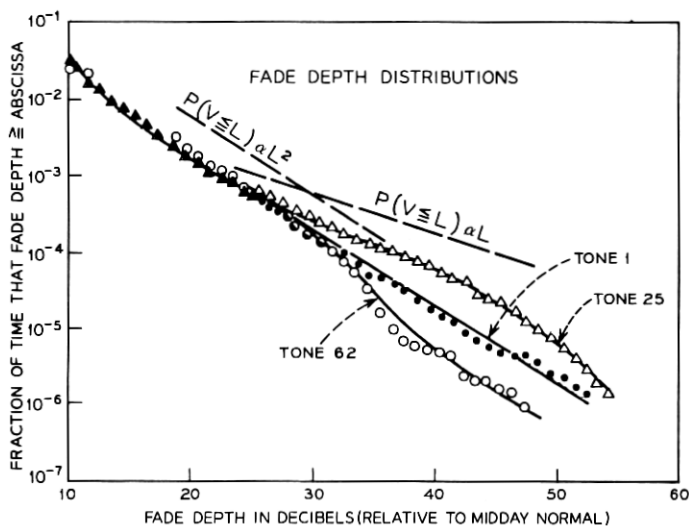

Fig. 7—Fade depth distributions for tones 1, 25, and 62 received on the horn reflector antenna.

Both distributions (1) and (2) are shown on Fig. 7 with slopes of a decade decrease in probability of occurrence per 10 and 20 dB, respectively.

For fade depths less than about 30 dB all three tones exhibit the L^2 dependence, indicating that the majority of the events at these levels were not due to dominant echo interference. For fade depths greater than 30 dB, tone 25 sustained significantly more deep fading and exhibited the L dependency. The indication was that at some time during the 5.1×10^6 seconds of the measurement period, the lower atmospheric structure was sufficiently stable and produced a dominant echo with appropriate amplitude and time delay (phase) resulting in substantial selective fading in the middle of the narrowband radio channel (tone 25). Studies of line-of-sight propagation at the same[3] and other microwave links[5,6] indicate that single dominant echo fading is not the typical multipath mechanism for overland fading. This period during dominant echo interference was assumed as atypical and was extracted from the total data base for special study (Section VIII). It is important to note, as indicated in Fig. 8, that the fade depth distributions for the same tones received on the dish antenna (located 19 feet 3 inches below the horn antenna) all exhibited the L^2 dependency. This reflects the strong spatial sensitivity of multipath fading and will be discussed further in Section VIII.
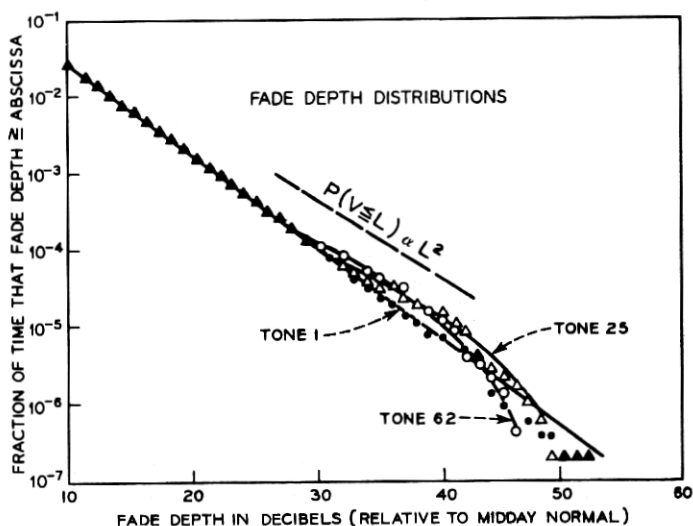

Fig. 8—Fade depth distributions for tones 1, 25, and 62 received on the dish antenna.

A day-by-day examination of the fading activity indicated that the atypical dominant echo event occurred on the morning of October 5 between 4 and 7:30 A.M.. With this time period removed from the data base the fade depth distribution for tone 25, shown in Fig. 9, exhibited more closely the L^2 dependency. The faded depth distribution of tone 62 remained unchanged because of the small sample size at the extremity of the narrowband.

Whereas the slope of the single-tone fade depth distribution curve gives information about the multipath fading process, the ordinate intercept gives a measure of the occurrence of such fading. Previous experience[1] at the same frequency and at approximately the same path length and path roughness indicates that the proportionality constant of equation (1) is about 0.5 which implies that $P(V \leq 0.032) \cong 5 \times 10^{-4}$ at the 30-dB fade depth $[-20 \log (0.032) = 30]$ as plotted in the figures. Figure 9 shows that the fading activity was below expectation at all fade depths; about 1/5 of that expected. This lack of observations was compensated for by using the condensed data base as discussed in Section IV. That is, we had 1/5 the number of fades, but we condensed the time base by five to compensate. This allows us to extrapolate these observations of frequency selective fading derived from a modest but, we believe, not atypical set
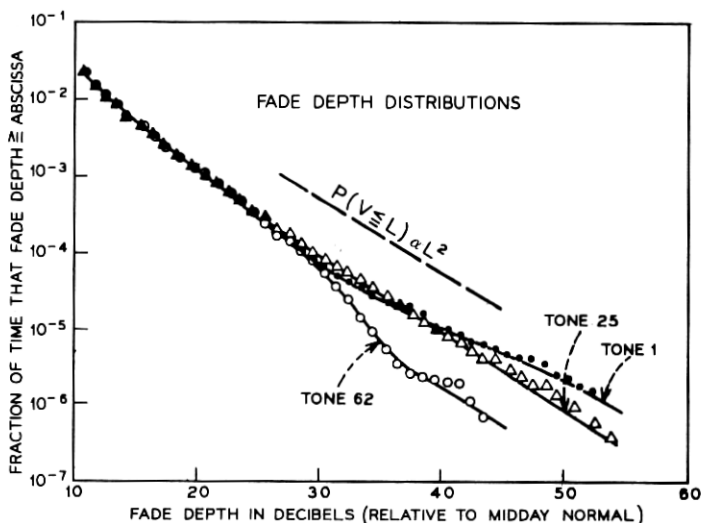

Fig. 9—Fade depth distributions for tones 1, 25, and 62 received on the horn reflector antenna for the entire 1970 measurement period excluding the fading activity of October 5.

of measurements during this late fall fading season to what is believed to be more representative of a typical summer fading month.

VI. SELECTIVITY CHARACTERIZATION OF MULTIPLE TONE ACTIVITY

To give a flavor of the variety and nature of the selective fading observed during the 1970 measurement period and to motivate the characterization of such events, two fading periods are presented in Figs. 10a and 10b. These time sequences of the channel transmission loss (displayed here as a continuous amplitude-frequency characteristic rather than discrete measurements) indicate the dynamics and dispersion of the channel. For figure compactness, the sequential scans of the tone field have arbitrary 0 dB reference; the absolute fade depth of tone 1 is indicated. The time between scans was 0.2 second. Event (a) was extremely rapid, and was preceded by 2 and followed by 6 days of near free-space propagation conditions. During the period shown in event (a), all tones in the narrowband channel were faded 20 dB. Event (b) was preceded by 9 days of free-space conditions and was followed by additional selective fading periods within the hour. For this early morning event the highly selective portion of the fade was superimposed on what appears to be a broader-band selective fade as indicated by the slopes of the amplitude characteristic before and after the events of greatest dispersion.

In event (a) the selectivity swept through the narrowband, suggesting the appearance of a very small echo with rapidly changing delay (phase), which maintained, at least approximately, a constant amplitude. In contrast, in event (b) the selectivity develops and dissipates in-band, suggesting a continual change in the relative amplitude of the echoes present. All of the highly selective fading events observed exhibited activity somewhere between these two extremes and the study of events such as these will undoubtedly sharpen our thinking about the mechanisms of multipath fading.

The choice of form of characterization of such selective fading events is bounded by the two constraints of generality and simplicity. Study of events like those shown in Fig. 10, and others, suggested that the amplitude-frequency characteristic most frequently exhibited either simple slopes or simple curvatures (or combinations of slopes and curvatures) and only for the deeper fades did higher-order structure (for example, cusps) occur. Therefore, the detailed variation across the amplitude-frequency characteristic was parameterized by monitoring the amplitudes of three symmetrically spaced reference tones as shown
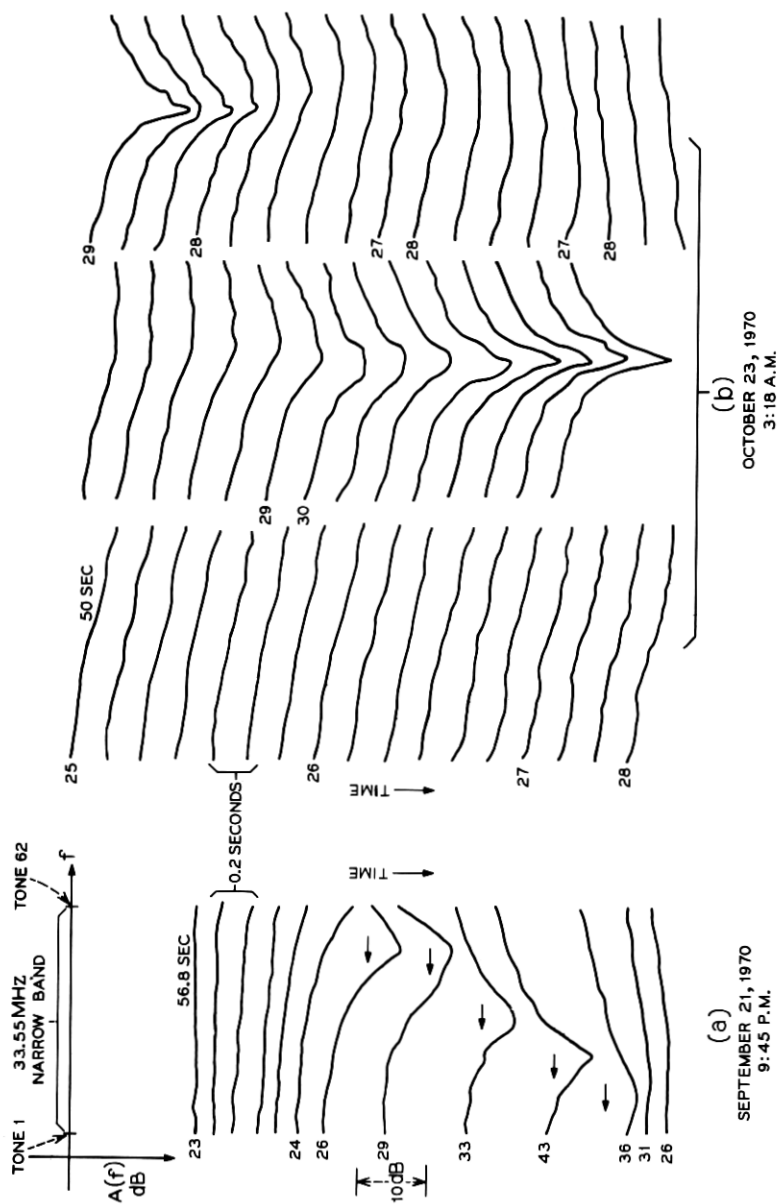
Fig. 10—Time sequential plots of selective faded amplitude-frequency characteristic. The fade depth of the lowest frequency tone (#1) is indicated when changes in amplitude occurred.

in Fig. 11. The three amplitudes, $A(f_1)$, $A(f_2)$, and $A(f_3)$, were used to construct the simple first difference

$$\Delta A = A(f_3) - A(f_1), \tag{3}$$

which is the linear amplitude distortion (slope) in dB across a narrow-band channel of width $f_3 - f_1 = 2\Delta f$, and the second difference

$$\frac{\Delta^2 A}{2} = \frac{A(f_1) + A(f_3)}{2} - A(f_2), \tag{4}$$

which is the quadratic amplitude distortion (curvature) in dB across the $2\Delta f$ channel. ΔA, $\Delta^2 A/2$, and $A(f_2)$ form a complete set; $A(f_2)$ is defined to be the fade depth of the event, $2\Delta f$ is the bandwidth parameter. For the example shown in Fig. 11, the fade depth is $A(f_2) = -34$ dB and for a bandwidth of $2\Delta f = 20.35$ MHz, the linear distortion is $\Delta A = 10$ dB and the quadratic distortion is $\Delta^2 A/2 = 6$ dB.

The 1.05×10^6 seconds of data were processed and the observed experimental distributions for $|\Delta A|$ and $|\Delta^2 A/2|$ were accumulated both for conditional and unconditional fade depths [conditioned on $A(f_2)$] as well as for seven different bandwidths ($2\Delta f = 1.65$ to 33.55 MHz). The results of this selectivity characterization are presented in the following sections in the order:

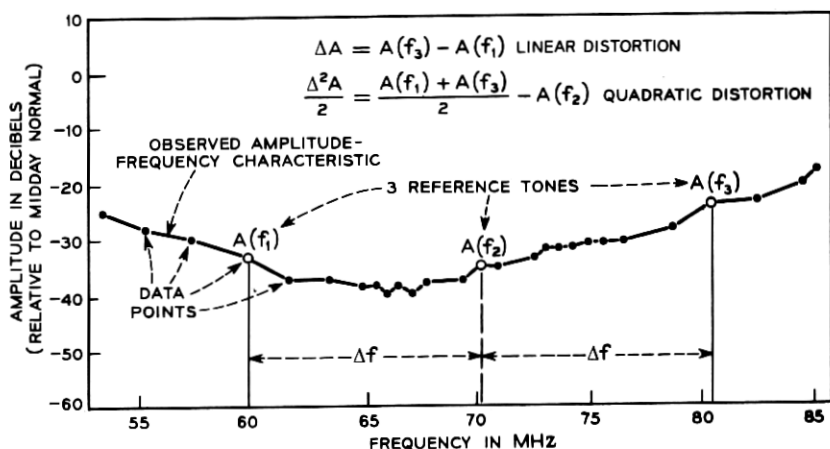(i) Unconditional linear and quadratic distortion for a bandwidth of 20.35 MHz,

Fig. 11—Selectivity characterization of the observed amplitude-frequency characteristic.

(*ii*) Conditional linear and quadratic distortion for 20.35 MHz,

(*iii*) Unconditional distortion for other bandwidths,

(*iv*) Crossplots of the above results showing growth in selectivity structure with bandwidth and fade depth.

6.1 *20.35-MHz Bandwidth*

The unconditional linear and quadratic distortion distributions for 20.35 MHz are shown in Fig. 12. The abscissa is the amount of distortion in dB and the ordinate is the fraction of time (1.05×10^6 seconds) that the linear or quadratic distortion equaled or exceeded the corresponding abscissa value. For example, $\Delta A \geq 15$ dB and $\Delta^2 A/2 \geq 9.5$ dB for 10^{-5} of the time (about 10 seconds). As indicated for smaller fractions of the time even greater distortion was observed. The roll-off at the tails below 10^{-6} is the result of too few samples. The data points below 10^{-4} can be approximated by lines with slopes of a decade of probability of occurrence per 10 dB of distortion and will be discussed in Section 6.2.

It is appropriate to comment here on the effects of quantization. Since the measured amplitude of each tone has a maximum uncertainty of ± 0.5 dB, there results a maximum uncertainty of ± 1 dB in both
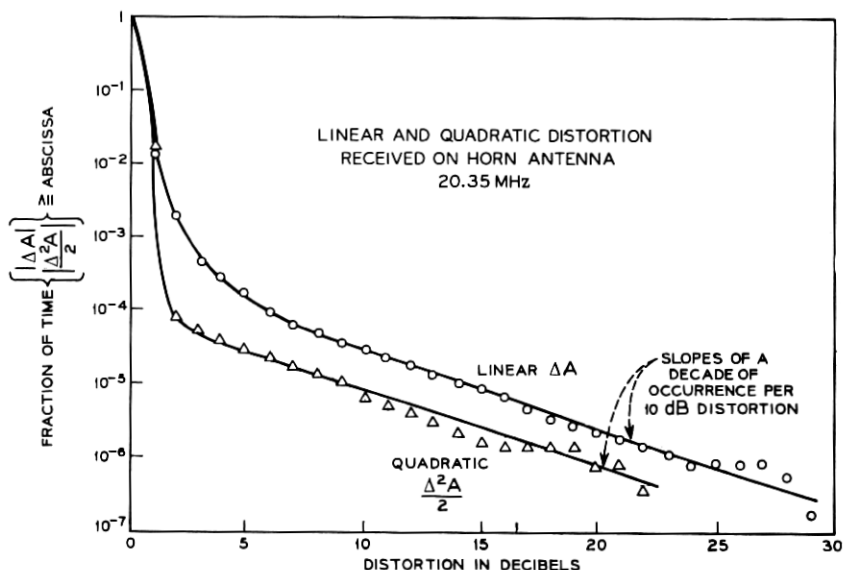
Fig. 12—Unconditional linear and quadratic distortion distributions for a bandwidth of 20.35 MHz.

linear and quadratic distortion parameters. Assuming that the error in each tone measurement is uniformly distributed about 0 dB (a reasonable assumption for a many-measurement statistic) results in an average error of 0 dB for the distortion parameters ΔA, and $\Delta^2 A/2$. Thus we conclude that the quantization effects are secondary and manifest themselves only at the distribution's tails where the samples are few. In addition, it is important to realize that for high-performance microwave systems the relevant fraction of time for propagation considerations of a single radio hop is in the range of 10^{-4} to 10^{-5}. For these fractions of time the data shows consistency.

The linear and quadratic distortion distributions for a 20.35-MHz bandwidth conditioned on the fade depth of the middle tone $[A(f_2)]$ are shown in Figs. 13 and 14, respectively. Note that the time base for each curve is different and is the total time the middle tone was faded the indicated amount. For example, for half of the 30-dB fading time (about 7.4 seconds) the linear distortion $\Delta A \geq 3.4$ dB and the quadratic distortion $\Delta^2 A/2 \geq 1.8$ dB. The point scatter of the linear distortion at the 25-dB level is difficult to explain; the irregular position of the 35-dB curve suggests that at (and below) these fade levels a simple linear distortion characterization parameter is an inadequate descriptor of the frequency selectivity in the narrowband channel. As anticipated, the distortion values increase with fade depth, particularly the quadratic distortion below the 30-dB level.

6.2 Other Bandwidths

By processing different sets of three reference tones, information regarding the bandwidth of the selective fading process was obtained.
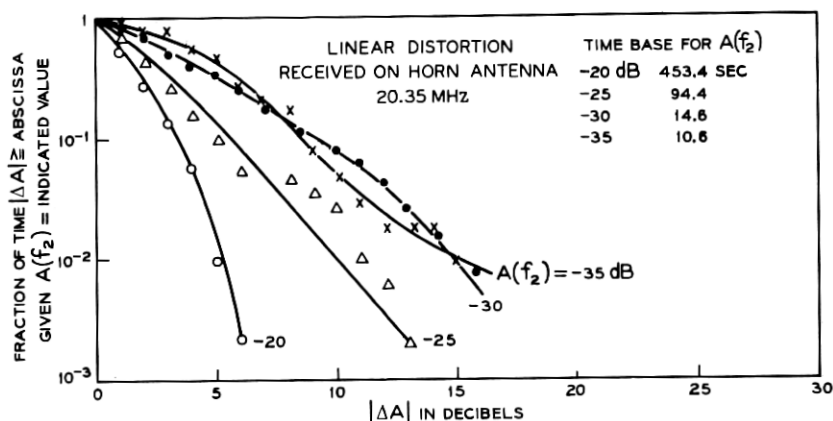

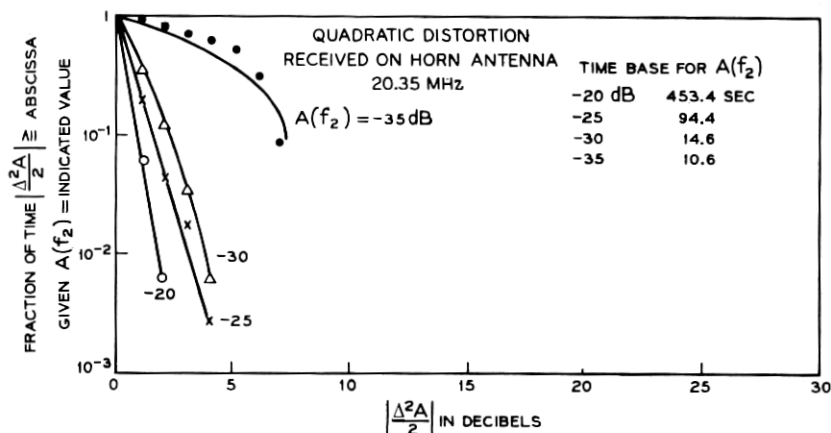Fig. 13—Conditional linear distortion distributions for 20.35 MHz.

Fig. 14—Conditional quadratic distortion distributions for 20.35 MHz.

Figure 15 shows a summary of the unconditional linear distortion distributions for different bandwidths and Fig. 16 indicates the quadratic distributions. Remembering again that the data below 10^{-6} are less reliable because of fewer samples, the linear distortion distribution shows good consistency for the different bandwidths. The quadratic distributions show more scatter; the unusual behavior of the quadratic distortion for the 33.55-MHz case indicates the inadequacy of characterizing the selective fading amplitude characteristic by monitoring three reference tones spanning a bandwidth as great as 33.55 MHz. For bandwidths less than 5 MHz the tones are highly correlated and the amplitude distortion parameters are smaller.

Both the linear and quadratic distortion curves for the larger bandwidths exhibit slopes of a decade decrease of probability for 10 dB increase in distortion. This is a general result for deeply faded signals and their differences when such quantities are expressed in dB.

To examine more closely the increase in amplitude distortion with increased bandwidth and fade depth, several crossplots of the previously shown results were constructed. Figure 17, a crossplot of Figs. 15 and 16, shows the growth in distortion as a function of channel bandwidth for 10^{-5} fraction of the time. As indicated, the distortion increases rapidly with increasing bandwidth up to about 5 MHz; beyond 5 MHz the increase is less. For the quadratic distortion the transition point appears to occur around 20 MHz.

Crossplots of Figs. 13, 14, and others (not shown) for 10^{-2} fraction of the middle reference tone $[A(f_2)]$ fade time give the results shown in Fig. 18 for bandwidths of 10.45 and 20.35 MHz. The growth in
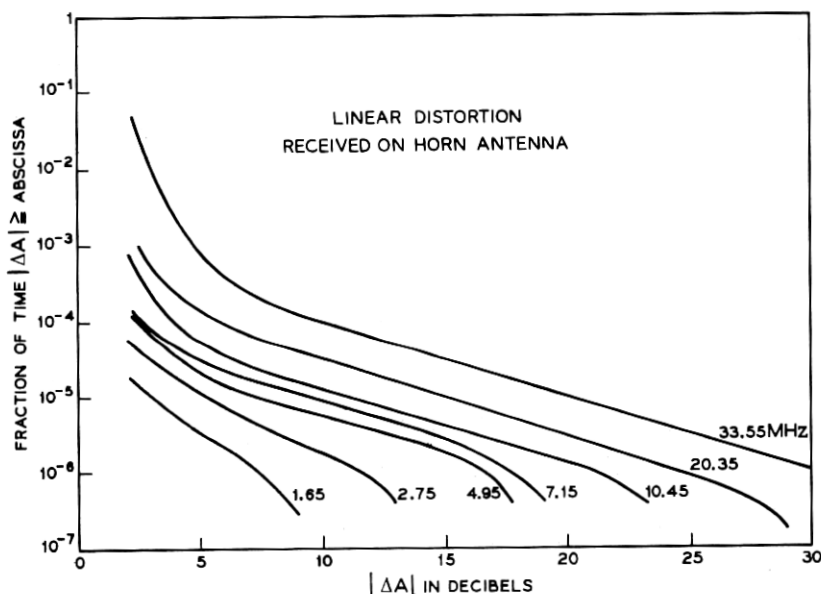
Fig. 15—Summary of unconditional linear distortion distributions for different bandwidths.

distortion is clearly a function of both fade depth and bandwidth. The dashed lines showing the estimated growth in the quadratic distortion below 30 dB were obtained by extrapolation of conditional distortion curves to the appropriate fade depths.

VII. AN ERROR ANALYSIS OF THE HIGHER-ORDER DISTORTION

As previously indicated, the selectivity structure increases with fade depth and monitoring the relative amplitudes of only three tones will not provide a complete description of the frequency selectivity for deep fades. In this section we discuss these higher-order selective effects and describe how a determination was made of the fade depth at which higher-order effects become significant.

This determination was made by making use of the multiple-tone amplitudes measured in the following way: For each amplitude-frequency characteristic measurement the three-term power series approximation was constructed

$$A(f) = A(f_2) + \frac{\Delta A}{2}\left(\frac{f - f_2}{\Delta f}\right) + \frac{\Delta^2 A}{2}\left(\frac{f - f_2}{\Delta f}\right)^2, \qquad (5)$$
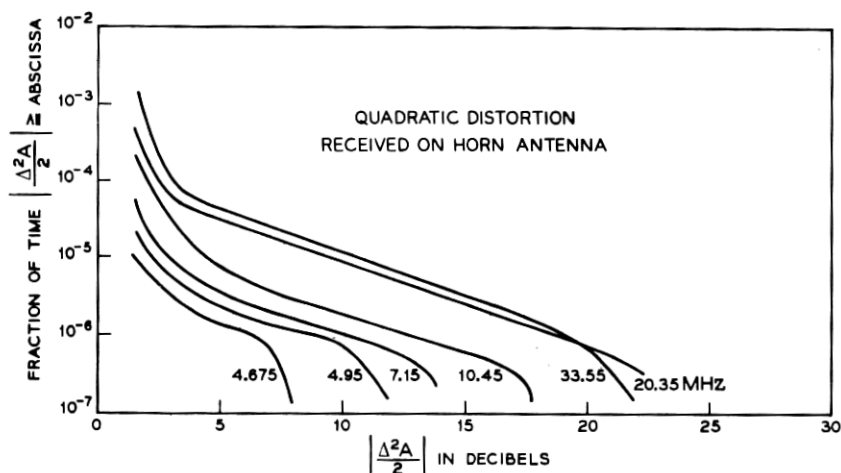
Fig. 16—Summary of unconditional quadratic distortion distributions for different bandwidths.

where ΔA and $\Delta^2 A/2$ are again the distortion parameters as defined in (3) and (4). Then by using the measured amplitudes, A^M, of tones (called here intertones) falling within the $2\Delta f$ bandwidth, the errors (deviations) between the measured values and the values calculated by the power series approximation (5) were found by
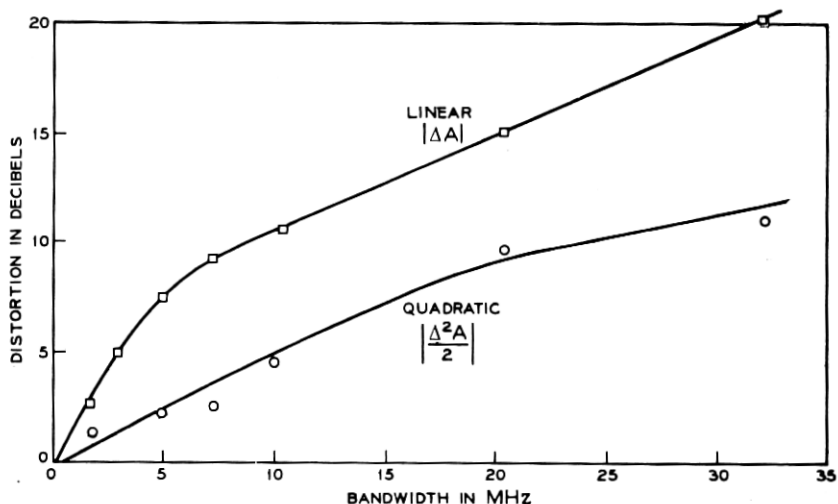

Fig. 17—Observed unconditional linear and quadratic distortions for 10^{-5} fraction of time for different bandwidths.
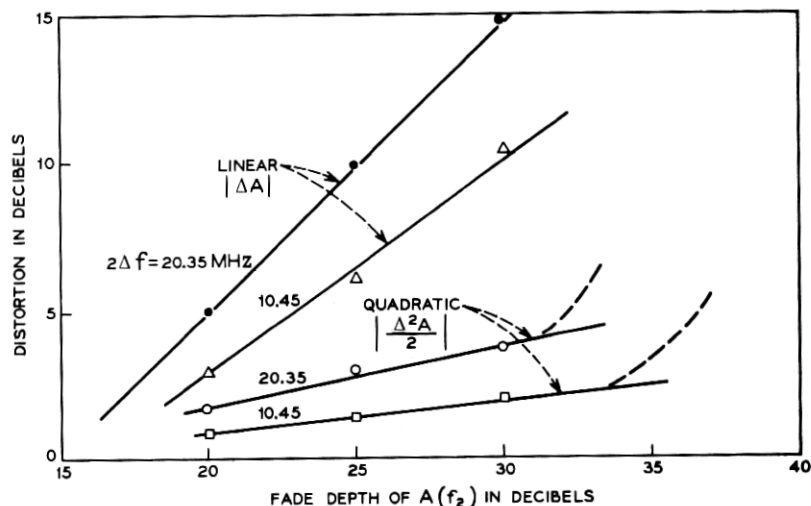
Fig. 18—Observed conditional linear and quadratic distortions for 10^{-2} fraction of the middle reference tone's fade time for 10.45 and 20.35 MHz.

$$E_i = E(f_i) = A^M(f_i) - A(f_i). \tag{6}$$

Figure 19 shows, for an instant in time, the observed selectivity, the power series approximation, and two of the intertone errors. The maximum of the absolute value of the set $\{E_i\}$ called MAX | ERROR | (maximum inband amplitude deviation) was monitored as a function
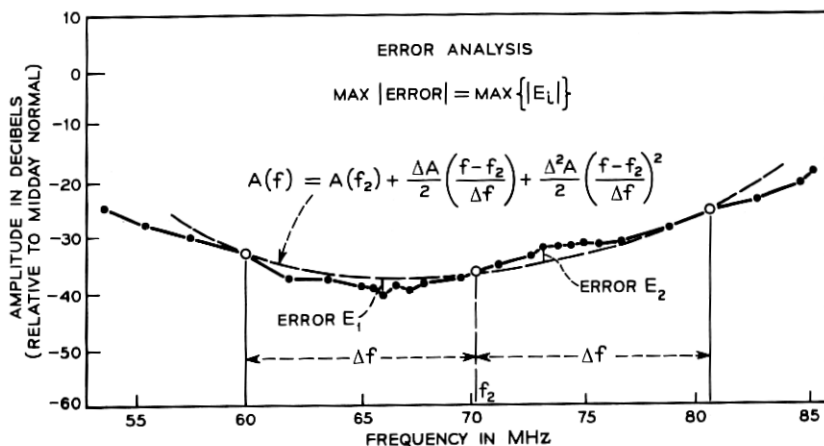
Fig. 19—Definition of errors as differences between the observed selectivity structure (solid line) and the power series approximation (dashed line).

of fade depth and tone spacing Δf. Figure 20 shows the experimental distribution of this MAX | ERROR | for a channel bandwidth of 20.35 MHz. Although the scatter of data is large (undoubtedly due to the higher-order selectivity structure), it is clear that for small fractions of the time the MAX | ERROR | can become significantly large (6 dB at 10^{-5} fraction time). The effect of decreasing the bandwidth is shown in Fig. 21. Figure 22, a crossplot of Fig. 21, indicates that, at 10^{-5} of the time, halving the bandwidth approximately halved the observed MAX | ERROR |. But, as indicated, the bandwidth would have to be limited to values considerably less than 5 MHz to limit MAX | ERROR | to less than 1 dB.

The large values of MAX | ERROR | occurred only during the deep selective fades, and we now explore these effects. The observed distribution of MAX | ERROR | for a bandwidth of 20.35 MHz conditioned on the fade depth of the middle reference tone is given in Fig. 23. Note again that the time base for each curve is different. As indicated, the MAX | ERROR | is a sensitive function of fade depth. Half of the time the middle reference tone $A(f_2)$ was faded 20, 25, or 30 dB, the MAX | ERROR | was less than 1 dB. But for the same
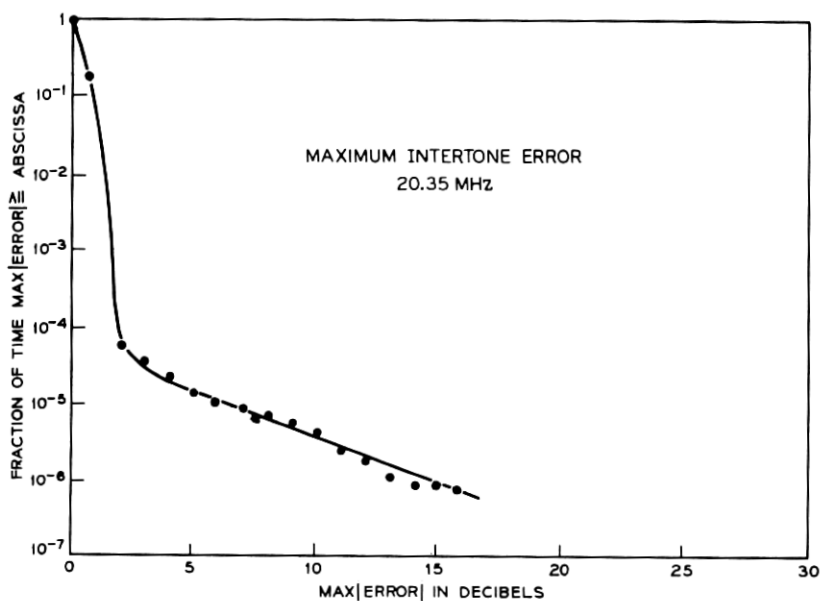

Fig. 20—Unconditional distribution of the MAX |ERROR| for a bandwidth of 20.35 MHz.
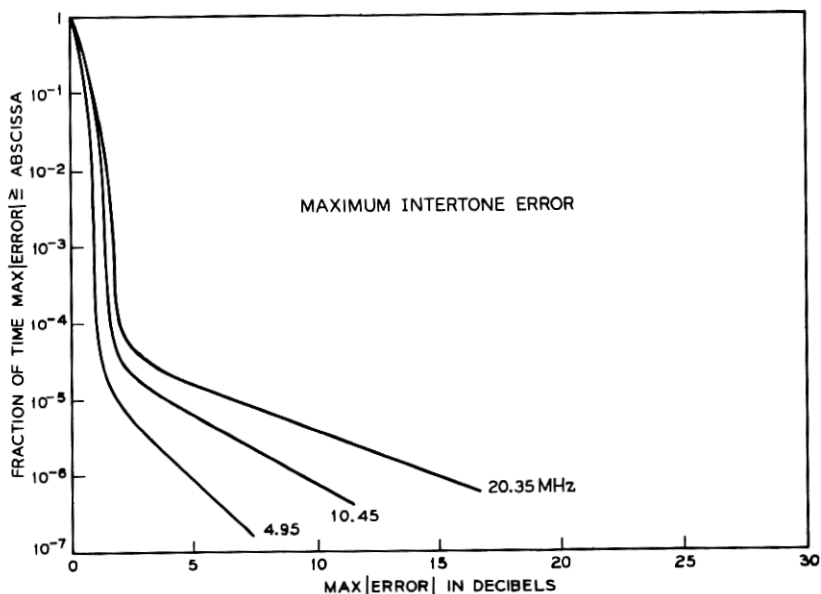
Fig. 21—Summary of unconditional distributions of MAX |ERROR| for additional bandwidths.

fraction of time when the middle tone was faded 35 dB, the MAX | ERROR | was greater than 2.5 dB. The same rapid growth in MAX | ERROR | below 30 dB was also observed for the other bandwidths as indicated in Fig. 24, which is for the 10^{-2} fraction of the middle reference tone's fade time. This figure indicates that for bandwidths from 5 to 20 MHz and fades not in excess of 30 dB, the three-term power series approximation constructed from the linear and quadratic distortion parameters approximates the actual channel to within 2 dB. Below 30 dB the selectivity structure is often greater than second order, and higher-order distortion parameters constructed from more reference tones are required to more precisely quantify the frequency selectivity of channel loss.

VIII. SPECIAL TOPICS

8.1 *Temporal Activity*

Although the physical process responsible for multipath fading may be of relative slow time scale, reflecting the huge inertia of the extended propagating medium, the faded microwave signal, which

is the vector sum of multiple echoes, may itself exhibit much greater rates of change. An example of this was indicated in Fig. 10a.

Figure 25 illustrates a particular fade, in which the dynamics of the linear distortion, quadratic distortion, and MAX | ERROR | for a 20.35-MHz bandwidth are displayed. Note that as the selectivity develops the distortion grows to significant values. The three-tone power series approximation initially matches the channel frequency selectivity character to within 1 dB. During the 58th second, however, the selectivity structure is of such high order (again see Fig. 10a) that the power series approximation fails substantially to match the amplitude structure, resulting in MAX | ERROR |s in excess of 6 dB. The 30-dB fading period for the middle reference tone $A(f_2)$ is shown and further supports the earlier observation of the inadequacy of using only three tones to monitor selective fading over bandwidths of a few tens of MHz for fades below 30 dB. The rates of change $(d/dt)(\Delta A) \sim 90$ dB/second and $(d/dt)(\Delta^2 A/2) \sim 60$ dB/second, which existed for only a fraction of a second, were the maximum observed during the 1970 measurement period.

8.2 Spatial Activity

The fading activity experienced by a dish antenna located 19 feet 3 inches below the horn antenna was also monitored throughout the measurement period. The results, less complete than those for the
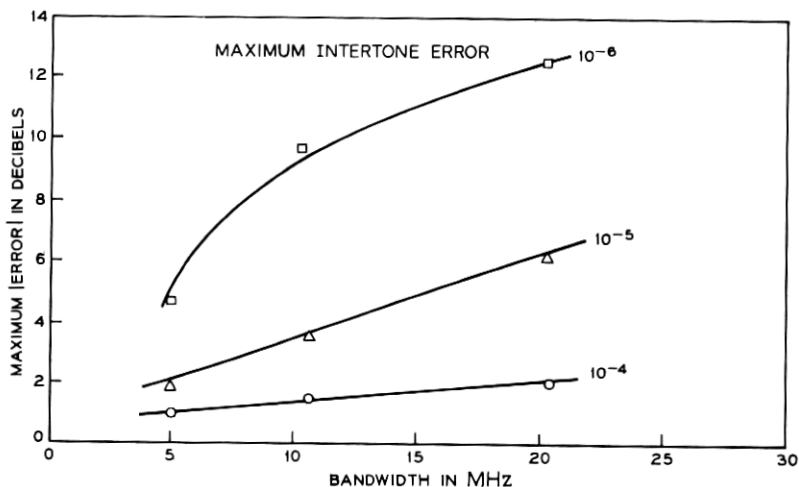

Fig. 22—A crossplot of Fig. 21 showing the observed MAX |ERROR| as a function of bandwidth for 10^{-4}, 10^{-5}, and 10^{-6} fractions of the time.
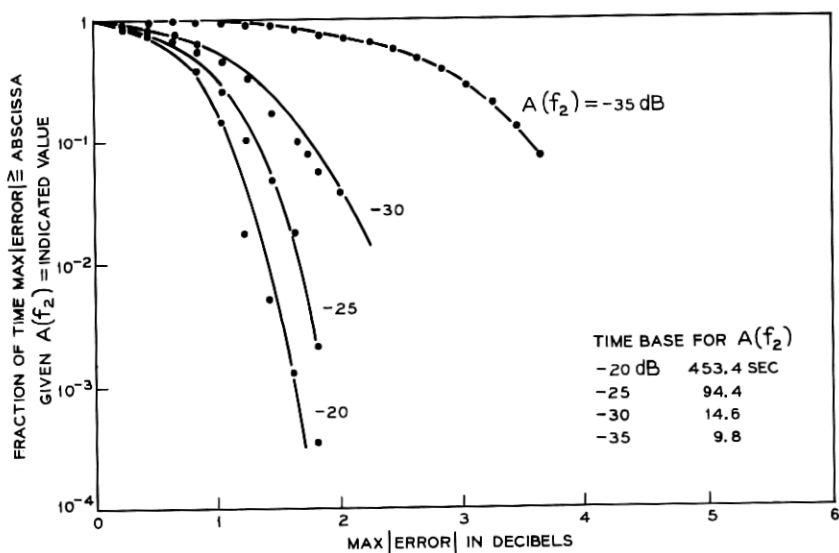
Fig. 23—Conditional distributions of MAX |ERROR| for a bandwidth of 20.35 MHz and different fade depths.

horn reflector because of fewer tones recorded (see Fig. 3), are shown in Fig. 26. These distributions also have slopes of a decade of probability per 10 dB of distortion for the main portion of the curves. The roll-off at the tails is a small samples effect. Comparing the selectivity characterization plots for the horn in Figs. 15 and 16 to the plots for the dish in Fig. 26, we see the same amount of selectivity structure. The
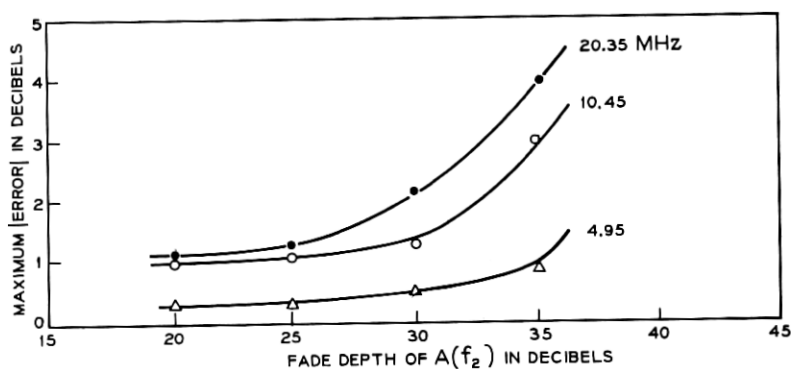
Fig. 24—Observed MAX |ERROR| for 10^{-2} fraction of the middle reference tone's fade time as a function of fade depth and bandwidth.
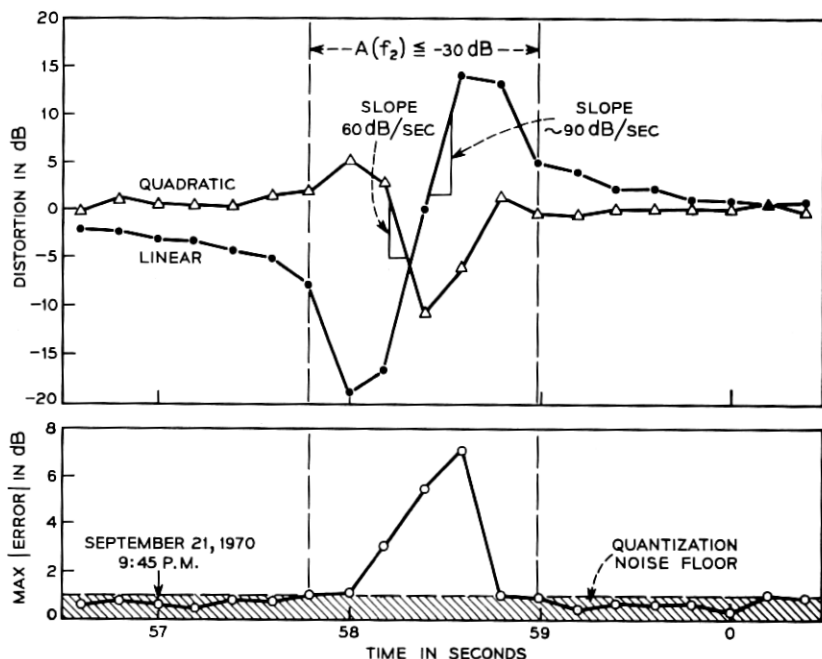
Fig. 25—Dynamics of the linear and quadratic distortion and the MAX |ERROR| for a bandwidth of 20.35 MHz. This is the event shown in Fig. 10a.

conclusion is that the selective fading structure as observed in a narrowband radio channel at these frequencies is insensitive to the beamwidth or to the precise vertical location of the antenna.

Although the joint activity of selective fading in the narrowband channels received on both antennas was not directly processed, examination of all significant fading periods showed very few simultaneous events with appreciable selectivity.

8.3 *The Atypical Event of October 5*

For completeness, the linear and quadratic distortion distributions were accumulated for the entire measurement period including the assumed atypical event of October 5. The distributions for a 20.35-MHz bandwidth are shown in Fig. 27. The distortion distributions for this inclusive period have the same slope as before (see Fig. 12), indicating that the frequency selective structure which occurred during this unusually long dominant echo period was similar to the selective structure occurring during the remainder of the experiment.
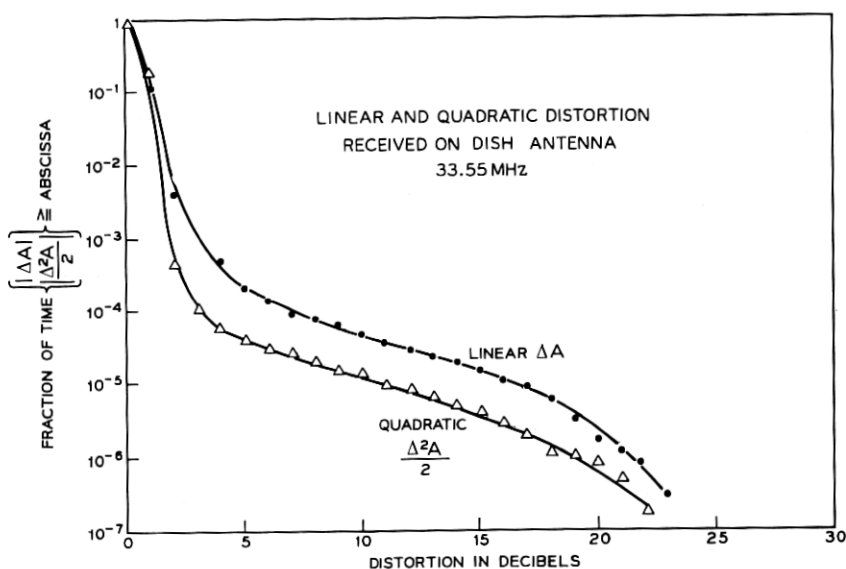
Fig. 26—Unconditional distributions of the linear and quadratic distortion received on the dish for a bandwidth of 33.55 MHz.
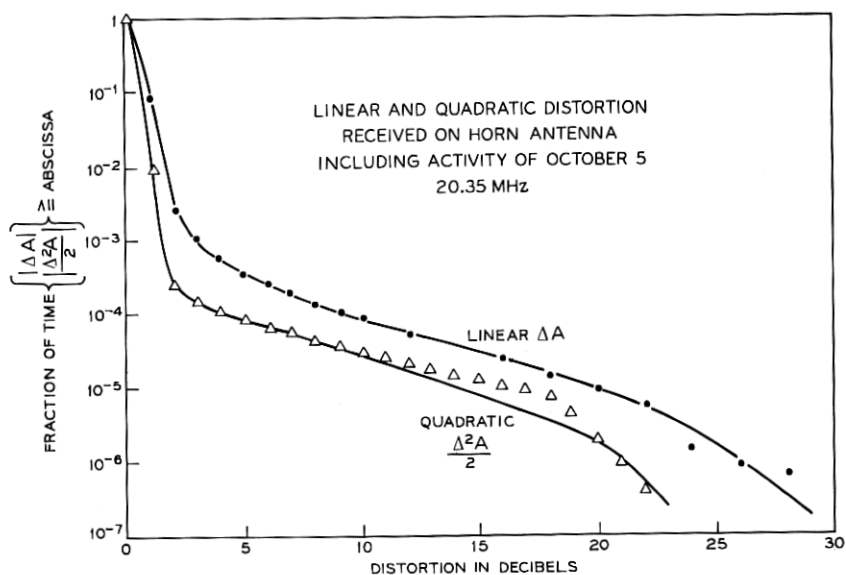

Fig. 27—Unconditional linear and quadratic distortion distributions for a bandwidth of 20.35 MHz and for the entire 1970 measurement period including the activity of October 5.

IX. ACKNOWLEDGMENTS

REFERENCES

1. Barnett, W. T., "Microwave Line-of-Sight Propagation With and Without Frequency Diversity," B.S.T.J., *49*, No. 8 (October 1970), pp. 1827–1871.
2. Kaylor, R. L., "A Statistical Study of Selective Fading of Super High Frequency Radio Signals," B.S.T.J., *32*, No. 5 (September 1953), pp. 1187–1202.
3. Lin, S. H., "Statistical Behavior of a Fading Signal," B.S.T.J., *50*, No. 10 (December 1971), pp. 3211–3270.
4. Babler, G. M., "Scintillation Effects at 4 and 6 GHz on a Line-of-Sight Microwave Link," IEEE Trans. Ant. and Prop., *AP-19*, No. 4 (July 1971), pp. 574–575.
5. Crawford, A. B., and Jakes, W. C., "Selective Fading of Microwaves," B.S.T.J., *31*, No. 1 (January 1952), pp. 68–90.
6. DeLange, O. E., "Propagation Studies at Microwave Frequencies by Means of Very Short Pulses," B.S.T.J., *31*, No. 1 (January 1952), pp. 91–103.